

## Synthesis of Isatins and Oxindoles Derivatives as SARS-CoV-2 Inhibitors Evaluated through Phenotypic Screening with Vero Cells

Cintia M. C. F. Lima,<sup>a,b</sup> Lúcio H. Freitas-Junior,<sup>c</sup> Carolina B. Moraes,<sup>c,d</sup>  
Cecília G. Barbosa,<sup>c,e</sup> Till Opatz<sup>f</sup> and Mauricio M. Victor<sup>✉</sup>\*,<sup>a,b</sup>

<sup>a</sup>Departamento de Química Orgânica, Instituto de Química, Universidade Federal da Bahia, Campus de Ondina, 40170-115 Salvador-BA, Brazil

<sup>b</sup>Centro Interdisciplinar de Energia e Ambiente (CIENAM), Universidade Federal da Bahia, Campus de Ondina, 40170-115 Salvador-BA, Brazil

<sup>c</sup>Departamento de Microbiologia, Instituto de Ciências Biomédicas, Universidade de São Paulo, 05508-000 São Paulo-SP, Brazil

<sup>d</sup>Departamento de Ciências Farmacêuticas, Universidade Federal de São Paulo, 09913-030 Diadema-SP, Brazil

<sup>e</sup>Universidade Municipal de São Caetano do Sul (USCS), Campus Centro, 09521-160 São Caetano-SP, Brazil

<sup>f</sup>Institute of Organic Chemistry, Johannes Gutenberg-University of Mainz, 55128 Mainz, Germany

To expand the variety of density functionalized compounds evaluated against severe acute respiratory syndrome coronavirus 2 (SARS-CoV-2), we decided to prepare new acetylated and disubstituted 3-hydroxy bis-oxindoles and isoindigos coupling compounds using known protocols. The corresponding isatin derivatives were synthesized by  $ZrCl_4/EtOH$ /reflux or  $HCl/AcOH$ /reflux coupling conditions using oxindole and functionalized isatins, furnishing new 3-hydroxy bis-oxindoles, which were dehydrated into new isoindigos. A total of 27 compounds bearing halogen, nitro and/or hydroxy groups on the isatin moiety at the 3-, 5- and 7-positions, were prepared, including 5 new 3-hydroxy bis-oxindoles and 3 new halogenated isoindigos prepared according to adapted procedures described in the literature. This library of nitrogen-isatin derivatives was evaluated against SARS-CoV-2 using a phenotypic screening assay. In this investigation, isatin derivatives **3d**, **3e**, **3h** and **3i** showed antiviral activity when tested at a single concentration. Compound **3e** showed antiviral activity against SARS-CoV-2 in the concentration-response assay; however, it showed cellular toxicity in Vero cells. The present study identified substituted isatins as a promising new starting point for the development of anti-SARS-CoV-2 agents.

**Keywords:** 3-hydroxy bis-oxindoles, isoindigos, isatins, SARS-CoV-2, phenotypic VERO essay

### Introduction

The severe acute respiratory syndrome coronavirus 2 (SARS-CoV-2) is the virus responsible for the transmission and symptoms of the COVID-19 (coronavirus disease 2019). It was first reported in Wuhan Province, China, in December 2019.<sup>1</sup> The infection has since spread worldwide, reaching as of September 2022, 608,000,000 cases and

over 6,500,000 deaths worldwide.<sup>2</sup> SARS-CoV-2 has been documented as the most infectious, fatal and pathogenic coronavirus after SARS-CoV (2002) and Middle East Respiratory Syndrome coronavirus (MERS-CoV, 2012) (SARS-CoV (800 deaths) and MERS-CoV (858 deaths)).<sup>3</sup> From the above data it is clear that SARS-CoV-2 is much more dangerous and virulent as compared to other coronaviruses. SARS-CoV-2 is a positive-sense single-stranded RNA virus (+ssRNA).<sup>4</sup> The similar names of SARS-CoV and SARS-CoV-2 were introduced by the scientific community due to the genome sequence similarity

\*e-mail: mmvictor@ufba.br

Editor handled this article: Brenno A. D. Neto (Associate)

of both coronaviruses, which could vary from 86%<sup>5</sup> until 89.1%.<sup>1</sup>

To date, some drugs have shown to have activity against SARS-CoV-2 *in vitro* and *in vivo*, with remdesivir<sup>®</sup> being the first small-molecule antiviral approved for COVID treatment by the US Food and Drugs Administration (FDA). Yet, clinical effects and efficacy of the drug remdesivir are still controversial.<sup>6-9</sup> Despite the development of successful new antivirals and vaccines for COVID, the development of new drugs for SARS-CoV-2 treatment continues. Several efforts are focused on the development of molecules that can inhibit the essential major polyprotein processing, 3CL<sup>pro</sup> (Type 3 chymotrypsin protease),<sup>10</sup> which is crucial for the viral replication.<sup>11</sup>

After the transcription of its genome, the beta-coronavirus genus produces a polypeptide of approximately 800 kDa, which is proteolytically cleaved to generate several proteins. This proteolytic processing is mediated by proteases such as PL<sup>pro</sup> (Papain-like protease) and 3CL<sup>pro</sup>. 3CL<sup>pro</sup> is the main protease found in the coronavirus. It consists of a 33.8 kDa cysteine protease which mediates the maturation of functional polypeptides involved in the assembly of the transcriptional machinery of viral replication. 3CL<sup>pro</sup> cleaves the polyprotein at 11 conserved sites, generating non-structural proteins that play an important role in viral replication. Furthermore, 3CL<sup>pro</sup> is located at the 3' end, exhibiting high variability levels.<sup>12-14</sup>

3CL<sup>pro</sup> plays an important role in polyproteins hydrolysis generating non-structural proteins (NSPs). Therefore, inhibitors of these proteases can block the generation of non-structural proteins. This enzyme is necessary for the proteolytic maturation of viral polyproteins (pp1a and pp1ab) to form the RNA replicase-transcriptase complex, which is essential for both viral transcription and replication processes.<sup>15,16</sup> These proteases are essential tools for the self-cleavage process and play a key-role in viral particle replication and infection, which makes it recognized as a high potential target for drugs that aim to control SARS-CoV-2 infection.<sup>17</sup> Now if we can covalently bind small molecules to this nucleophilic center, this will lead to the deactivation of 3CL<sup>pro</sup>, inhibiting its binding to ACE2 (angiotensin-converting-enzyme) receptor of the human body causing no infection by SARS-CoV-2.<sup>18</sup>

ACE2 recognition by the S protein enables SARS-CoV-2 invasion. Therefore, the decrease in the activity and expression of ACE2 in the membrane of the cell reduces the entry capacity and inflammatory activity of the virus.<sup>19</sup> Considering this information, the ideal compound would be one that has the ability of destabilizing the interaction between S protein and ACE2 receptor, causing the inhibition of virus entry as well as interrupting the activity

of enzymes involved in SARS-CoV-2 replication cycle.

Several small molecules screened from various chemical libraries have been identified as potent SARS-CoV-2 protease inhibitors.<sup>20</sup> However, some of these small molecules may be unsuitable for easy structural modification. Consequently, pharmacophoric scaffolds, which are easy to synthesize and chemically modify must be explored. In this direction, isatin derivatives occupy a prominent position as synthetic platform for drug design to an antiviral candidate.<sup>21</sup> For example, *N*-alkylated isatin derivatives **1a** and **1b** showed high half-maximal inhibitory concentration (IC<sub>50</sub>) values against SARS-CoV,<sup>22</sup> which resembles to the SARS-CoV-2 with 86% of similarity (Figure 1). Computational modeling revealed that steric effects from *N*-alkylated side chain was crucial for inhibitory potency, as well as the hydrophobicity and presence of electron withdrawing groups such as bromo and nitro on the isatin core. Zhou *et al.*<sup>23</sup> also reported isatin derivatives substituted at the *N*-1 and C-5 positions. In their studies, the *N*-alkylated C-5 substituted carboxamide group **2** was the most active compound against SARS-CoV 3C-like protease. According to the authors, the carboxamide assists the occupation of the active site through hydrogen bonding interactions. Due to this prominent position of isatin derivatives by its easily chemical modifications and antiviral activities, we decided to synthesize new 3-hydroxy bis-oxindoles, isoindigos and evaluate them, together with the isatins used in their preparation, against SARS-CoV-2 coronaviruses.

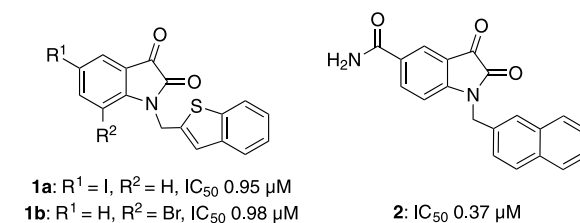


**Figure 1.** Structures of isatin derivatives with inhibitory activity against SARS coronavirus.

## Experimental

### Chemistry

#### Materials and methods

Solvents and reagents were purchased from commercial suppliers (Sigma-Aldrich, Darmstadt, Germany; Alfa Aesar, Kandel, Germany; ABCR ACROS Organics, Schwerte, Germany and Fischer Scientific, Schwerte, Germany). Nuclear magnetic resonance (NMR) spectra were recorded using the following spectrometers from Bruker (Ettlingen, Germany) in deuterated solvents from

Deutero and Sigma-Aldrich: Avance-III HD 300:  $^1\text{H}$  NMR (300 MHz),  $^{13}\text{C}$  NMR (75.5 MHz), Avance-II 400:  $^1\text{H}$  NMR (400 MHz),  $^{13}\text{C}$  NMR (100.6 MHz) and Bruker DRX 400  $^1\text{H}$  NMR (400 MHz),  $^{13}\text{C}$  NMR (100.6 MHz). The chemical shifts were referenced to the residual solvent signal ( $\text{CDCl}_3$ :  $\delta_{\text{H}} = 7.26$  ppm,  $\delta_{\text{C}} = 77.16$  ppm;  $\text{CD}_3\text{SOCHD}_2$ :  $\delta_{\text{H}} = 2.50$  ppm,  $\delta_{\text{C}} = 39.52$  ppm;  $\text{C}_5\text{D}_5\text{N}$ :  $\delta_{\text{H}} = 8.74$  ppm,  $\delta_{\text{C}} = 150.35$  ppm). The evaluation and assignment of the spectra was achieved using the software MestReNova from Mestrelab Research.  $^1\text{H}$  NMR data are reported as follows: chemical shift (parts *per* million, ppm), multiplicity (s = singlet, d = doublet, t = triplet, dd = doublet of doublets, dt = doublet of triplets, m = multiplet), coupling constant (*J*) in hertz (Hz), integration and assignment. High-performance liquid chromatography (HPLC) analysis was recorded on HPLC-UV system Shimadzu (Kyoto, Japan) equipped with binary pump DGU-20A5 Prominence, with a diode array detector (DAD) SPD-M20A. Electrospray ionization high resolution mass spectrometry (ESI-HRMS) spectra were recorded on Waters Q-TOF-Ultima III instrument from Waters (Milford, USA) with a dual source and a suitable external calibrant. IR spectra were recorded on routine Fourier transform infrared (FTIR) spectrometer (Bruker Optics Tensor 27, Ettlingen, Germany) using a diamond ATR unit. The evaluation of the spectra was achieved using the software Opus 6.5 from Bruker. FTIR device from Shimadzu IRAffinity-1 (Kyoto, Japan) with compressed tablets of anhydrous potassium bromide and FTIR-ATR on the equipment model Cary 630 Agilent equipped with attenuated total reflectance (ATR) with diamond crystal cell and deuterated triglycine sulfate detector (DTGS). Melting point ranges were determined with IA9000 series digital melting point apparatus from ThermoFischer (Waltham, USA) and MQAPF-302 instrument (Cotia, Brazil) and were uncorrected.

#### Synthesis of isatin and acetylated isatin derivatives

Compounds 5-bromo-1*H*-indoline-2,3-dione (**3b**), 5-chloro-1*H*-indoline-2,3-dione (**3c**), 5-nitro-1*H*-indol-2,3-dione (**3d**), 5,7-dibromo-1*H*-indoline-2,3-dione (**3e**), 5,7-dichloro-1*H*-indoline-2,3-dione (**3f**), 5-chloro-7-bromo-1*H*-indoline-2,3-dione (**3g**), *N*-acetylindoline-2,3-dione (**3h**), *N*-acetyl-5-bromoindoline-2,3-dione (**3i**), *N*-acetyl-5-chloroindoline-2,3-dione (**3j**), *N*-acetyl-5-nitroindoline-2,3-dione (**3k**), 3-hydroxy-(3,3'-biindoline)-2,2'-dione (**4a**), 5-bromo-3-hydroxy-(3,3'-biindoline)-2,2'-dione (**4b**), 5-chloro-3-hydroxy-(3,3'-biindoline)-2,2'-dione (**4c**), and 3-hydroxy-5-nitro-(3,3'-biindoline)-2,2'-dione (**4d**) were synthesized as described in the literature. For more details, see Supplementary Information (SI) section.

#### General procedures for synthesis of 3-hydroxy bis-oxindoles

(*E*)-(3,3'-Biindolinylidene)-2,2'-dione (**5a**), (*E*)-5-bromo-(3,3'-biindolinylidene)-2,2'-dione (**5b**), (*E*)-5-chloro-(3,3'-biindolinylidene)-2,2'-dione (**5c**), and (*E*)-5-nitro-(3,3'-biindolinylidene)-2,2'-dione (**5d**) were synthesized as described in the literature. For more details, see SI section.

(i) Method *i*:<sup>24</sup> indole-2,3-dione derivatives (**3a-3g**; **3i-3j**, 0.5 mmol), indolin-2-one (**6**, 0.5 mmol) and  $\text{ZrCl}_4$  (23 mg, 0.1 mmol) were heated in anhydrous ethanol (4 mL) under reflux overnight. The mixture was slowly cooled to room temperature. The colored solids precipitated and were collected by filtration, then washed by a small amount of anhydrous ethanol to deliver undehydrated product 3-hydroxy-3,3'-biindoline-2,2'-dione (**4a-4i**). The obtained compounds were dried in the oven.

(ii) Method *ii*:<sup>25</sup> indolin-2-one (**6**, 0.5 mmol) and substituted indole-2,3-dione (**3a-3g**; **3i-3j**, 0.5 mmol) were dissolved in glacial acetic acid and one drop of concentrated hydrochloric acid was added. The solution was stirred under reflux overnight. The resultant mixture was concentrated under vacuum. Toluene was added to aid the removal of glacial acetic acid. Ethyl acetate was added to the residue, the suspension was filtered under reduced pressure, washed with chilled ethyl acetate, and dried in oven. The target compounds were obtained usually as a purple red powder.

#### 5,7-Dibromo-3-hydroxy-(3,3'-biindoline)-2,2'-dione (**4e**)

Purple solid; mp > 390 °C; yield 73%; IR (ATR)  $\nu/\text{cm}^{-1}$  3145, 1703, 1609, 1555, 1445, 1335, 1309, 1156, 865, 604;  $^1\text{H}$  NMR (400 MHz,  $\text{DMSO}-d_6$ )  $\delta$  10.91 (s, 1H), 10.28 (s, 1H), 7.61 (d, 1H, *J* 1.8 Hz), 7.57 (d, 1H, *J* 7.3 Hz), 7.31 (t, 1H, *J* 7.6 Hz), 7.06 (t, 1H, *J* 7.5 Hz), 6.92 (s, 1H), 6.80 (d, 1H, *J* 7.7 Hz), 6.04 (s, 1H), 4.03 (s, 1H);  $^{13}\text{C}$  NMR (100 MHz,  $\text{DMSO}-d_6$ )  $\delta$  176.2, 173.7, 143.4, 141.7, 134.2, 131.8, 128.9, 126.7, 125.6, 125.1, 121.4, 113.0, 109.2, 102.9, 76.2, 51.6; HRMS (APCI) *m/z*, calcd. for  $\text{C}_{16}\text{H}_8\text{Br}_2\text{N}_2\text{O}_2$  [*M* -  $\text{H}_2\text{O}$ ]: 417.8953, found: 417.8951.

#### 5,7-Dichloro-3-hydroxy-(3,3'-biindoline)-2,2'-dione (**4f**)

Purple solid; mp > 390 °C; yield 61%; IR (ATR)  $\nu/\text{cm}^{-1}$  3202, 1730, 1693, 1619, 1454, 1162, 742;  $^1\text{H}$  NMR (400 MHz,  $\text{DMSO}-d_6$ )  $\delta$  11.04 (s, 1H), 10.27 (s, 1H), 7.58 (d, 1H, *J* 7.3 Hz), 7.42 (d, 1H, *J* 2.0 Hz), 7.32 (t, 1H, *J* 7.8 Hz), 7.06 (t, 1H, *J* 7.2 Hz), 6.93 (s, 1H), 6.81 (d, 1H, *J* 7.7 Hz), 5.91 (d, 1H, *J* 1.6 Hz), 4.05 (s, 1H);  $^{13}\text{C}$  NMR (100 MHz,  $\text{DMSO}-d_6$ )  $\delta$  176.9, 173.9, 143.6, 139.9, 131.7, 129.2, 129.1, 126.9, 125.6, 125.3, 122.6, 121.6, 114.7, 109.4, 76.2, 51.7; HRMS (APCI) *m/z*, calcd. for  $\text{C}_{16}\text{H}_8\text{Cl}_2\text{N}_2\text{O}_2$  [*M* -  $\text{H}_2\text{O}$ ]: 329.9963, found: 329.9959.

**7-Bromo-5-chloro-3-hydroxy-(3,3'-biindoline)-2,2'-dione (4g)**

Red solid; mp > 390 °C; yield 63%; IR (ATR)  $\nu / \text{cm}^{-1}$  3144, 3068, 1703, 1614, 1451, 1335, 1307, 868, 746;  $^1\text{H}$  NMR (400 MHz, DMSO- $d_6$ )  $\delta$  10.91 (s, 1H), 10.28 (s, 1H), 7.57 (d, 1H,  $J$  7.3 Hz), 7.50 (d, 1H,  $J$  2.0 Hz), 7.31 (t, 1H,  $J$  7.7 Hz), 7.05 (t, 1H,  $J$  7.5 Hz), 6.93 (s, 1H), 6.80 (d, 1H,  $J$  7.7 Hz), 5.92 (s, 1H), 4.03 (s, 1H);  $^{13}\text{C}$  NMR (100 MHz, DMSO- $d_6$ )  $\delta$  176.3, 173.3, 143.0, 141.0, 131.3, 131.0, 128.5, 126.3, 125.2, 124.7, 122.3, 121.0, 108.8, 102.1, 75.8, 51.1; HRMS (APCI)  $m/z$ , calcd. for  $\text{C}_{16}\text{H}_8\text{BrClN}_2\text{O}_2$  [M -  $\text{H}_2\text{O}$ ]: 373.9458, found: 373.9456.

**N-Acetyl-5-bromo-3-hydroxy-(3,3'-biindoline)-2,2'-dione (4i)**

Brown solid; mp > 390 °C; yield 61%; IR (ATR)  $\nu / \text{cm}^{-1}$  3345, 1746, 1714, 1620, 1470, 1299, 1188, 1164, 832;  $^1\text{H}$  NMR (300 MHz, DMSO- $d_6$ )  $\delta$  10.32 (s, 1H), 8.01 (d, 1H,  $J$  8.7 Hz), 7.67 (d, 1H,  $J$  7.3 Hz), 7.52 (dd, 1H,  $J$  8.7, 2.2 Hz), 7.52 (dd, 1H,  $J$  8.7, 2.2 Hz), 7.35 (t, 1H,  $J$  7.7 Hz), 7.23 (s, 1H), 7.12 (t, 1H,  $J$  7.2 Hz), 6.80 (d, 1H,  $J$  7.7 Hz), 6.25 (d, 1H,  $J$  2.2 Hz), 4.20 (s, 1H), 2.64 (s, 3H);  $^{13}\text{C}$  NMR (75 MHz, DMSO- $d_6$ )  $\delta$  177.3, 174.2, 170.7, 144.0, 139.6, 133.3, 130.2, 129.7, 127.1, 126.9, 125.2, 122.2, 118.3, 117.1, 110.0, 75.6, 53.8, 26.6; HRMS (ESI)  $m/z$ , calcd. for  $\text{C}_{18}\text{H}_{13}\text{BrN}_2\text{O}_4$ : 400.0059, found: 400.0057.

**N-Acetyl-5-chloro-3-hydroxy-(3,3'-biindoline)-2,2'-dione (4j)**

Rose solid; mp > 390 °C; yield 56%; IR (ATR)  $\nu / \text{cm}^{-1}$  3338, 1743, 1712, 1617, 1403, 1183, 1076, 1030, 834;  $^1\text{H}$  NMR (300 MHz, DMSO- $d_6$ )  $\delta$  10.30 (s, 1H), 8.06 (d, 1H,  $J$  8.8 Hz), 7.66 (d, 1H,  $J$  7.4 Hz), 7.44-7.27 (m, 2H), 7.22 (s, 1H), 7.15-7.03 (m, 1H), 6.79 (d, 1H,  $J$  7.7 Hz), 6.10 (d, 1H,  $J$  2.3 Hz), 4.20 (s, 1H), 2.63 (s, 3H);  $^{13}\text{C}$  NMR (75 MHz, DMSO- $d_6$ )  $\delta$  177.3, 174.1, 170.5, 143.8, 139.1, 130.3, 129.8, 129.6, 129.0, 127.0, 125.1, 123.8, 122.1, 117.8, 109.9, 75.5, 53.6, 26.4; HRMS (ESI)  $m/z$ , calcd. for  $\text{C}_{16}\text{H}_{11}\text{ClN}_2\text{O}_3$  [M - Ac]: 314.0458, found: 314.0453.

**General procedure for synthesis of isoindigos**

Undehydrated 3-hydroxy bis-oxindoles (0.2 mmol) from general procedures A or B were placed in an inert atmosphere under reflux overnight in dry toluene (2 mL) in acidic medium (one drop of sulfuric acid). The crude was vacuum filtered, washed with ethyl acetate (2 x 2 mL) and dried under vacuum to furnish the corresponding isoindigos as colored solids.

**(E)-5,7-Dibromo-(3,3'-biindolinylidene)-2,2'-dione (5e)**

Purple solid; mp > 390 °C; yield 45%; IR (ATR)  $\nu / \text{cm}^{-1}$  1700, 1609, 1444, 1307, 1151, 1017, 864;  $^1\text{H}$  NMR (400 MHz, DMSO- $d_6$ )  $\delta$  11.32 (s, 1H), 11.04 (s, 1H), 9.33

(t, 1H,  $J$  5.6 Hz), 9.03 (d, 1H,  $J$  7.8 Hz), 7.82 (s, 1H), 7.39 (t, 1H,  $J$  7.6 Hz), 7.00 (t, 1H,  $J$  7.8 Hz), 6.84 (d, 1H,  $J$  7.9 Hz); HRMS (APCI)  $m/z$ , calcd. for  $\text{C}_{16}\text{H}_8\text{Br}_2\text{N}_2\text{O}_2$ : 417.8953, found: 317.8944.

**(E)-5,7-Dichloro-(3,3'-biindolinylidene)-2,2'-dione (5f)**

Purple solid; mp > 390 °C; yield 53%; IR (KBr)  $\nu / \text{cm}^{-1}$  3020, 2779, 1778, 1753, 1718, 1456, 1396, 1053, 771, 754;  $^1\text{H}$  NMR (400 MHz, DMSO- $d_6$ )  $\delta$  11.43 (s, 1H), 11.08 (s, 1H), 9.36 (s, 1H), 9.15 (s, 1H), 7.66 (d, 1H,  $J$  8.0 Hz), 7.59 (s, 1H), 7.12 (d, 1H,  $J$  8.0 Hz), 6.79 (d, 1H,  $J$  8.0 Hz);  $^{13}\text{C}$  NMR (100 MHz, DMSO- $d_6$ )  $\delta$  170.1, 169.2, 163.6, 145.8, 141.5, 137.1, 132.4, 131.8, 129.1, 128.2, 126.5, 126.1, 125.0, 121.5, 115.3, 109.8; HRMS (APCI)  $m/z$ , calcd. for  $\text{C}_{16}\text{H}_8\text{Cl}_2\text{N}_2\text{O}_2$ : 329.9963, found: 329.9960.

**(E)-7-Bromo-5-chloro-(3,3'-biindolinylidene)-2,2'-dione (5g)**

Red solid; mp > 390 °C, yield 60%; IR (KBr)  $\nu / \text{cm}^{-1}$  3186, 1703, 1614, 1450, 1337, 1308, 1180, 1161, 868, 608;  $^1\text{H}$  NMR (400 MHz, Pyr- $d_5$ )  $\delta$  12.84 (s, 1H), 12.45 (s, 1H), 9.82 (d, 1H,  $J$  1.9 Hz), 9.68 (d, 1H,  $J$  8.1 Hz), 7.67 (s, 1H), 7.39 (t, 1H,  $J$  7.6 Hz), 7.09 (t, 1H,  $J$  7.8 Hz), 7.00 (d, 1H,  $J$  7.8 Hz); HRMS (APCI)  $m/z$ , calcd. for  $\text{C}_{16}\text{H}_8\text{BrClN}_2\text{O}_2$ : 373.9458, found: 373.9451.

**Biological assays****Cell lines**

Vero CCL-81 (ATTC) cells were cultured in high glucose DMEM medium (Sigma-Aldrich) supplemented with 10% heat-inactivated fetal bovine serum (FBS) (Thermo Scientific, Waltham, USA) and 100 U mL $^{-1}$  of penicillin and 100  $\mu\text{g}$  mL $^{-1}$  Streptomycin (Thermo Scientific) at 37 °C with 5% CO $_2$ .

**Virus strain**

All procedures involving the SARS-CoV-2 virus were performed in the level 3 biosafety laboratory of the Institute of Biomedical Sciences of the University of São Paulo. The SARS-CoV-2 virus used in this study (HIAE-02: SARS-CoV-2/SP02/human/2020/ARB, GenBank Accession No. MT126808.1) was isolated from a nasopharyngeal sample of a confirmed COVID-19 patient at Hospital Israelita Albert Einstein, São Paulo (SP) Brazil.<sup>26</sup>

**Phenotypic screening with SARS-CoV-2**

For phenotypic screening of compounds, 2000 Vero CCL-81 (ATCC) cells were seeded *per well* in 384-well plates in high glucose Dulbecco's Modified Eagle Medium (DMEM) (Sigma-Aldrich, St. Louis, USA) supplemented with 10% heat-inactivated fetal bovine serum (Thermo

Scientific) and 100 U mL<sup>-1</sup> of penicillin and 100 µg mL<sup>-1</sup> of Streptomycin (Thermo Scientific). Cells were incubated for 24 h at 37 °C with 5% CO<sub>2</sub>. Compounds were diluted to 20 mM in dimethylsulfoxide (DMSO).

Before performing cell treatment, compounds were diluted 33.33× in phosphate-buffered saline (PBS), and 10 µL from each well was transferred to assay plates, thus having a final dilution factor of 200×. Initially the compounds were tested at a single concentration of 10 µM. Chloroquine (Sigma-Aldrich) was used as viral inhibition control in concentration-response curves, starting at 50 µM, with 10-concentration points and 2-fold dilutions. Compounds were also tested on a dose-response curve in which they were serially diluted and manually transferred to a 384-well polypropylene plate (Greiner Bio-One, Frickenhausen, Germany) containing sterile phosphate-buffered saline (PBS) pH 7.4, for a final dilution factor of 33.3. Then, 10 µL from each well in the compound plate was transferred to the assay plate containing cells, followed by the addition of SARS-CoV-2 viral particles to the cells at 0.1 multiplicity of infection (MOI) in 10 µL DMEM high glucose *per* well. After viral adsorption, high glucose DMEM medium supplemented with 6% fetal bovine serum was added. After 33 h of incubation at 37 °C, 5% CO<sub>2</sub> the plate was fixed in 4% paraformaldehyde in PBS pH 7.4 and subjected to indirect immunofluorescence detection of viral cell infection.<sup>27,28</sup> Three independent trials were performed.

For the detection of SARS-CoV-2 viral infection, the hyperimmune serum of a COVID-19 convalescent patient diluted 1:1000 in 5% bovine serum albumin (BSA, Sigma-Aldrich, St. Louis, USA) in PBS (v/v) was used as the primary antibody. After incubation, the wells were washed and a solution containing Alexa488-conjugated goat anti-human IgG (Thermo Fisher Scientific, Waltham, MA, USA) and 5 µg mL<sup>-1</sup> DAPI (4',6-diamidino-2-phenylindole; Sigma-Aldrich, St. Louis, MO, USA) diluted 1:1000 in 5% BSA (v/v) was added to each well.

Image acquisition was performed on the Operetta High Content Imaging System (PerkinElmer, Waltham, MA, USA) using a 20× magnification objective and image analysis was performed using Harmony software (PerkinElmer), version 3.5.2. The analysis consisted of identification and counting of Vero CCL-81 cells based on nuclear targeting and viral infection based on cytoplasmic staining detected by the immunofluorescence assay. The infection rate (IR) was calculated as the ratio of the number of infected cells to the number of total cells counted in each well. Cell survival rate was calculated as the number of cells counted in each well divided by the average number of cells in the positive control wells (DMSO-treated infected cells), multiplied by 100. Antiviral activity was determined by normalizing the IR

to the control negative (infected and uninfected cells treated with DMSO) as described. Concentration response curves were plotted using normalized activity and cell survival at each concentration. These two parameters were used to calculate EC<sub>50</sub> and CC<sub>50</sub> concentration, concentrations of compounds that reduce infection rate and cell survival by 50%, respectively, compared to untreated infected controls of each compound using GraphPad Prism version 9.0.<sup>29</sup>

## Results and Discussion

### Chemistry

The synthesized compounds were divided into three classes based on their structural complexity. Class 1 comprised isatins **3a-3k** with different substituents on the aromatic ring in the C-5 and/or C-7 position, as well as a *N*-acetyl protecting group. In this class we observed no *N*-acetylation (Ac<sub>2</sub>O, reflux) when a C-7 substituent (Br, Cl or NO<sub>2</sub>) was present. Class 2 consisted of 3-hydroxy bis-oxindoles **4a-4g**, **4i** and **4j**, which may be viewed as a 3-hydroxylated two 3,3'-linked oxindoles. Finally, class 3 (isoindigos **5a-5g**) were compounds structurally similar to class 2, except by an 3,3'-exocyclic double bond joined both oxindole structures. The structures of class 1-3 compounds are given in Figure 2. Of the 27 compounds prepared to this investigation, 19 members have been reported in the literature (see SI section for more details).

Our synthetic strategy to synthesize new disubstituted 3-hydroxy bis-oxindoles **4e-4g** and isoindigos **5e-5g** was based on known coupling methodologies described in the literature. In this direction, oxindole **6** was reacted with isatins **4e-4g** using ZrCl<sub>4</sub> in refluxing ethanol<sup>24</sup> (method *i*) or HCl in refluxing acetic acid<sup>25</sup> (method *ii*, Scheme 1). However, under both conditions no synthesis of isoindigos **5e-5g** were accomplished, and only the new intermediates 3-hydroxy bis-oxindoles **4e-4g** were obtained (Table 1). We reasoned those results due strong withdrawing effect of two halogen substituents on isatin moiety, which would make coordination of the hydroxyl group less effective and dehydration more difficult. The 3-hydroxy intermediates obtained were easily identified by NMR analysis: HO-C3-**H** was displayed at δ 4.03-4.05 ppm for **4e-4g** and at δ 4.19-4.22 ppm for acetylated **4h** and **4i**, while hydroxylated C3 was displayed ranging δ 76.2-75.6 ppm. We also observed during our synthetic efforts that *N*-acetyl protecting group on isatin partner were normally removed under coupling conditions, except when monohalogenated isatins **3i** and **3j** were coupled employing the method *ii*, leading to new **4i** and **4j** compounds, respectively. Finally, 3-hydroxy bis-oxindoles **4e-4g** were dehydrated under more

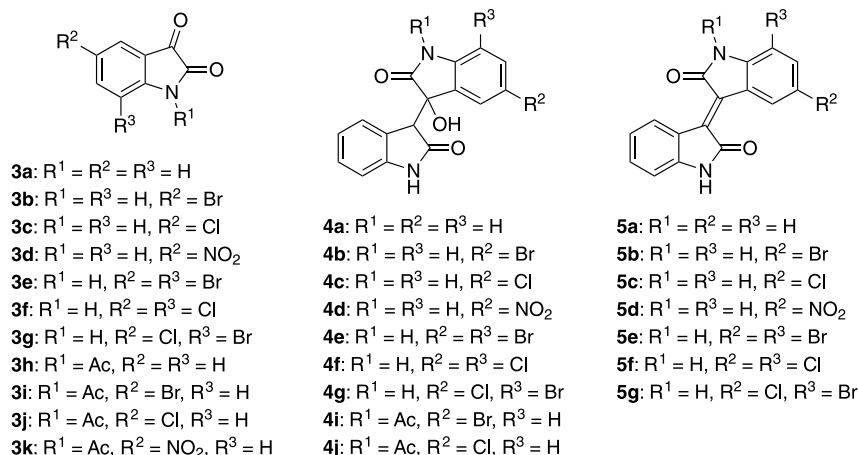
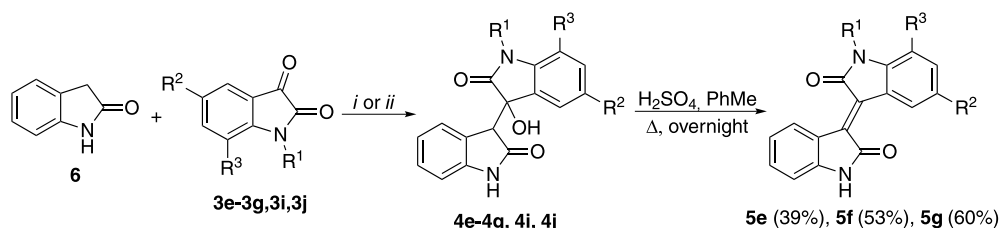


**Figure 2.** Compounds synthesized and evaluated against SARS-CoV-2.



**Scheme 1.** Synthetic pathway to new 3-hydroxy bis-oxindoles: (i) ZrCl<sub>4</sub>, EtOH, reflux, overnight, (ii) HCl conc., AcOH, reflux, overnight; and their dehydration to new isoindigos.

**Table 1.** New 3-hydroxy bis-oxindoles **4e-4g**, **4i** and **4j** synthesized

entry	R <sup>1</sup>	R <sup>2</sup>	R <sup>3</sup>	Compound	Yield / %
1	H	Br	Br	<b>4e</b>	method <i>i</i> : 73 method <i>ii</i> : 72
2	H	Cl	Cl	<b>4f</b>	method <i>i</i> : 61 method <i>ii</i> : 58
3	H	Cl	Br	<b>4g</b>	method <i>i</i> : 63 method <i>ii</i> : 45
4	Ac	Br	H	<b>4b</b> <b>4i</b>	method <i>i</i> : 18 <sup>a</sup> method <i>ii</i> : 61
5	Ac	Cl	H	<b>4c</b> <b>4j</b>	method <i>i</i> : 56 <sup>b</sup> method <i>ii</i> : 37

<sup>a</sup>Acetyl protecting group was removed and **4b** was obtained; <sup>b</sup>acetyl protecting group was removed and **4c** was obtained.

acidic conditions to furnished desired new isoindigos **5e-5g**, respectively, in moderate yields.

### Biological evaluation

#### Phenotypic assay with SARS-CoV-2

A high content screening assay (HCS) was designed to evaluate compounds that inhibit infection and cytotoxicity in Vero cells infected with a SARS-CoV-2 isolate.<sup>28</sup> The potential antiviral activity of 27 compounds against SARS-CoV-2 in Vero CCL-81 cells was evaluated. For this, an initial screening was performed, and the compounds were tested at a single concentration of 10 μM, as shown in Table 2.

**Table 2.** Anti SARS-CoV-2 activity by Vero CCL-81 cells-high content screening-at 10 μM (CS: cell survival; AA: antiviral activity)

Compound	CS / %	AA / %
<b>3a</b> (isatin)	109.38	25.05
<b>3b</b>	169.37	45.11
<b>3c</b>	51.15	30.46
<b>3d</b>	97.10	66.30
<b>3e</b>	79.54	64.92
<b>3f</b>	75.16	31.78
<b>3g</b>	95.26	35.49
<b>3h</b>	64.19	76.28
<b>3i</b>	91.39	61.48
<b>3j</b>	98.35	-9.70
<b>3k</b>	76.97	33.56
<b>4<sup>a</sup></b>	94.93	17.87
<b>4b</b>	102.57	21.66
<b>4c</b>	103.13	37.12
<b>4d</b>	96.76	6.17
<b>4e</b>	44.07	100.03
<b>4f</b>	54.78	12.47
<b>4g</b>	97.52	1.74
<b>4i</b>	107.94	23.20
<b>4j</b>	40.18	-7.33
<b>5a</b>	100.05	18.56
<b>5b</b>	98.15	42.70
<b>5c</b>	110.64	40.08
<b>5d</b>	102.95	47.53
<b>5e</b>	97.15	22.47
<b>5f</b>	104.47	6.96
<b>5g</b>	101.33	2.35
Chloroquine	121.81	96.96

Compounds that show antiviral activity greater than 60% and cell survival greater than 75% in the primary screening at a concentration of 10  $\mu\text{M}$  (**3d**, **3e**, **3h** and **3i**, Figure 3) were tested in dose-response, with an initial concentration of 100  $\mu\text{M}$  (Figure 4). These compounds belong to class 1 of isatins, with different substituents on the aromatic ring at the C5 and/or C7 position and/or acetylation of nitrogen. Compound **3e** showed activity against SARS-CoV-2 in the dose-response assay, however it showed cellular toxicity in Vero cells (Table 3).

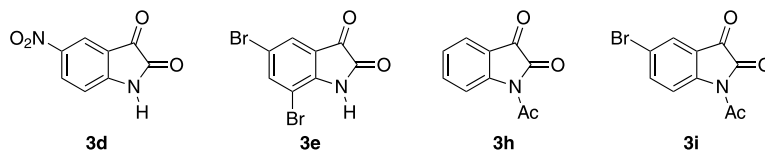


**Figure 3.** Compounds with antiviral activity in the primary screening against SARS-CoV-2.

**Table 3.** Inhibitory activities of compounds tested in concentration-response

Compound	EC <sub>50</sub> / $\mu\text{M}$	CC <sub>50</sub> / $\mu\text{M}$	SI
<b>3d</b>	>10	>10	1
<b>3e</b>	3.6	4.1	1.1
<b>3h</b>	>10	>10	1
<b>3i</b>	>10	>10	1

EC<sub>50</sub>: half maximum effective concentration; CC<sub>50</sub>: half maximum cytotoxic concentration; SI: selectivity index (CC<sub>50</sub>/EC<sub>50</sub>).

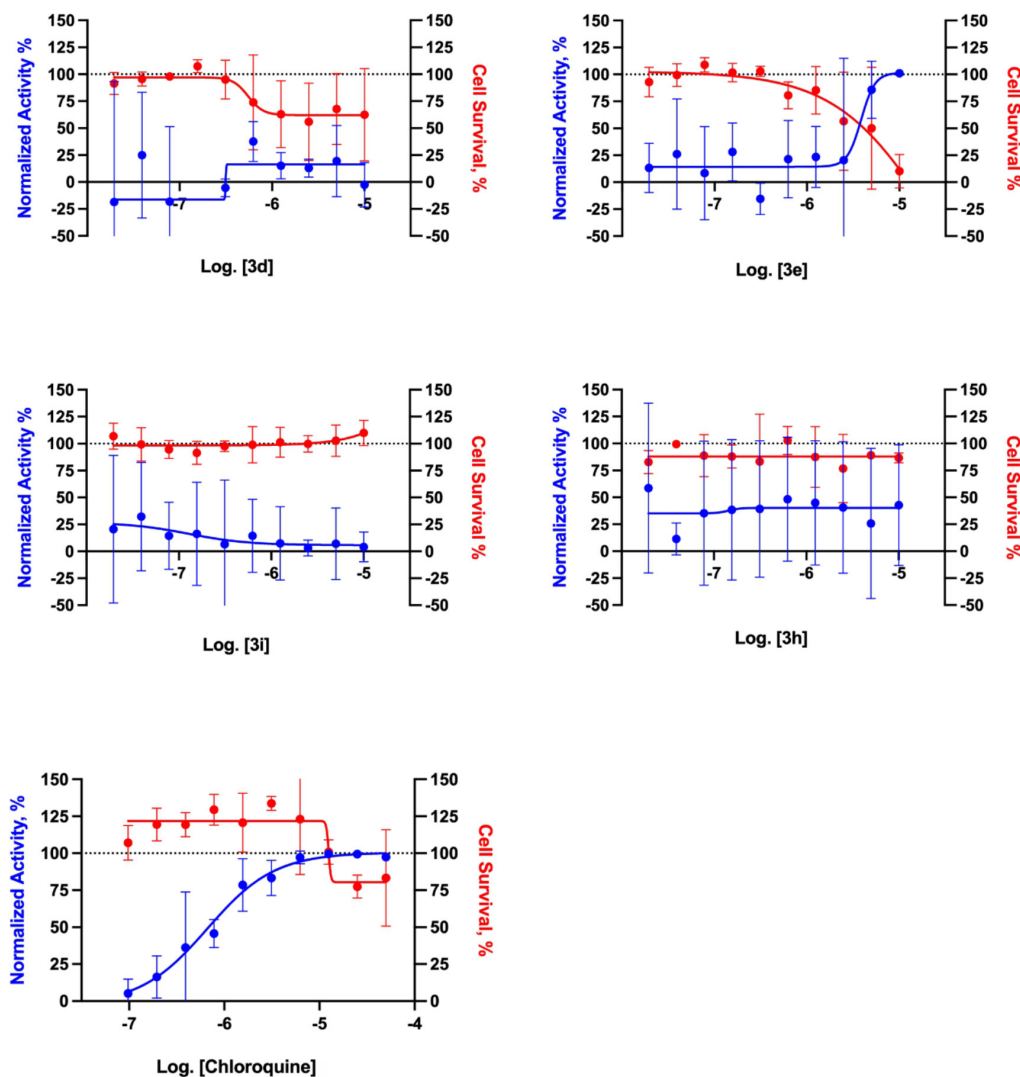


**Figure 4.** SARS-CoV-2 antiviral concentration-response curves for selected compounds. Chloroquine (CQ) was used as a positive control for viral infection inhibition. Represented *in vitro* antiviral activity (blue curves) and cytotoxic activity against Vero cells (red curves) against SARS-CoV-2. Three independent experiments were carried out.

## Conclusions

This investigation allowed the synthesis of 8 new isatin derivatives (5 new 3-hydroxy bis-oxindoles **4e-4g**, **4i** and **4j** and 3 new isoindigos **5e-5g**) in moderate yields, contributing to the expansion of this important derivative synthesis strategy. In addition, another 19 known compounds were prepared and all compounds were evaluated for their SARS-CoV-2 count properties through tests employing Vero cells.

Unfortunately, all the new compounds were found to be inactive against COVID-19 disease by the Vero cells evaluation. Among the other compounds evaluated, the brominated isatin derivatives (**3d** and **3i**), another which contain the nitro group (**3d**) and the *N*-acetylated isatin **3h**, showed the best antiviral activities by initial screening. Among active isatins, compound **3e** showed activity against SARS-CoV-2 in the dose-response assay, however it showed cellular toxicity in Vero cells. An important observation regarding structure-activity seems to be simplicity: while the 5,7-dibrominated **3e** and 5-nitro **3d** isatins showed antiviral activity, the respective 3-3' conjugated brominated derivatives **4e** and **5e** and with nitro group **4d** and **5d** showed lower activities. These results are in agreement with previous results described in the literature, where isatins showed previously promise of antiviral activity as an inhibitor of SARS-CoV-2 main protease (3CL<sup>pro</sup> or M<sup>pro</sup>), both *in silico* and *in vitro*.<sup>30-32</sup> However, despite the 3-hydroxy 5,7-dibrominated bisoxindole derivative **4e** showing high antiviral activity, it showed high cellular toxicity. The promising results of antiviral activity obtained with the simplest isatin derivatives **3d**, **3e**, **3h** and **3i** show that more detailed investigations need to be carried out.

## Supplementary Information

Supplementary data are available free of charge at <http://jbcs.sbq.org.br> as PDF file.

## Acknowledgments

The authors would like to acknowledge CIENAM, CNPq (by INCT E&A) and C.M.C.F.L. thanks CAPES PrInt/UFBA for fellowship. Debora de Andrade Santana (UNEB, Salvador) is grateful for HPLC analysis. This study was supported by CAPES - grant No. 88887.505029/2020-00. C.G.B. received a scholarship from CAPES (process No. 88887.643352/2021-00).

## Author Contributions

Cintia M. C. F. Lima was responsible for organic synthesis work; Lúcio H. Freitas-Junior for coordination of biological assays work; Carolina B. Moraes for biological assays work; Cecília G. Barbosa for biological assays work, contributions to manuscript writing; Till Opatz for coordination of organic synthesis work, contributions to manuscript writing; Mauricio M. Victor for coordination of organic synthesis work, contributions to manuscript writing.

## References

- Zhou, P.; Yang, X.-L.; Wang, X. G.; Hu, B.; Zhang, L.; Zhang, W.; Si, H.-R.; Zhu, Y.; Li, B.; Huang, C.-L.; Chen, H.-D.; Chen, J.; Luo, Y.; Guo, H.; Jiang, R.-D.; Liu, M. Q.; Chen, Y.; Shen, X. R.; Wang, X.; Zheng, X.-S.; Zhao, K.; Chen, Q.-J.; Deng, F.; Liu, L.-L.; Yan, B.; Zhan, F.-X.; Wang, Y.-Y.; Xiao, G.-F.; Shi, Z.-L.; *Nature* **2020**, *579*, 270. [Crossref]
- World Health Organization (WHO); *WHO Coronavirus Disease (COVID-19) Dashboard*, <https://covid19.who.int/>, accessed on 16<sup>th</sup> September 2022.
- Lee, P.-I.; Hsueh, P.-R.; *J. Microbiol., Immunol. Infect.* **2020**, *53*, 365. [Crossref]
- Satija, N.; Lal, S. K.; *Ann. N. Y. Acad. Sci.* **2007**, *1102*, 26. [Crossref]
- Chan, J. F.-W.; Kok, K.-H.; Zhu, Z.; Chu, H.; To, K. K.-W.; Yuan, S.; Yuen, K.-W.; *Emerging Microbes Infect.* **2020**, *9*, 221. [Crossref]
- Gupte, V.; Hegde, R.; Sawant, S.; Kalathingal, K.; Jadhav, S.; Malabade, R.; Gogtay, J.; *BMC Infect. Dis.* **2022**, *22*, 1. [Crossref]
- Mei, M.; Tan, X.; *Front. Mol. Biosci.* **2021**, *8*, 671263. [Crossref]
- Wang, Y.; Zhang, D.; Du, G.; Du, R.; Zhao, J.; Jin, Y.; Fu, S.; Gao, L.; Cheng, Z.; Lu, Q.; Hu, Y.; Luo, G.; Wang, K.; Lu, Y.; Li, H.; Wang, S.; Ruan, S.; Yang, C.; Mei, C.; Wang, Y.; Ding, D.; Wu, F.; Tang, X.; Ye, X.; Ye, Y.; Liu, B.; Yang, J.; Yin, W.; Wang, A.; Fan, G.; Zhou, F.; Liu, Z.; Gu, X.; Xu, J.; Shang, L.; Zhang, Y.; Cao, L.; Guo, T.; Wan, Y.; Qin, H.; Jiang, Y.; Jaki, T.; Hayden, F. G.; Horby, P. W.; Cao, B.; Wang, C.; *Lancet* **2020**, *395*, 1569. [Crossref]
- Beigel, J. H.; Tomashek, K. M.; Dodd, L. E.; Mehta, A. K.; Zingman, Z. S.; Kalil, A. C.; Hohmann, E.; Chu, H. Y.; Luetkemeyer, A.; Kline, S.; De Castilla, D. L.; Finberg, R. W.; Dierberg, K.; Tapson, V.; Hsieh, L.; Patterson, T. F.; Paredes, R.; Sweeney, D. A.; Short, W. R.; Touloumi, G.; Lye, D. C.; Ohmagari, N.; Oh, M.-d.; Ruiz-Palacios, G. M.; Benfield, T.; Fätkenheuer, G.; Kortepeter, M. G.; Atmar, R. L.; Creech, B.; Lundgreen, J.; Babiker, A. G.; Pett, S.; Neaton, J. D.; Burgess, T. H.; Bonnett, T.; Green, M.; Makowski, M.; Osinusi, A.; Nayak, S.; Lane, H. C.; *N. Engl. J. Med.* **2020**, *383*, 1813. [Crossref]

10. Ullrich, S.; Nitsche, C.; *Bioorg. Med. Chem. Lett.* **2020**, *30*, 127377. [Crossref]
11. Leyssen, P.; De Clercq, E.; Neyts, J.; *Antiviral Res.* **2008**, *78*, 9. [Crossref]
12. Shagufta; Ahmad, I.; *Eur. J. Med. Chem.* **2021**, *213*, 113157. [Crossref]
13. Qamar, M. T. U.; Alqahtani, S. M.; Alamri, M. A.; Chen, L.-L.; *J. Pharm. Anal.* **2020**, *10*, 313. [Crossref]
14. Anand, K.; Ziebuhr, J.; Wadhvani, P.; Mesters, J. R.; Hilgenfeld, R.; *Science* **2003**, *300*, 1763. [Crossref]
15. Song, L.-G.; Xie, Q.-X.; Lao, H.-L.; Lv, Z.-Y.; *Infect. Dis. Poverty* **2021**, *10*, 28. [Crossref]
16. Mouffouk, C.; Mouffouk, S.; Mouffouk, S.; Hambaba, L.; Haba, H.; *Eur. J. Pharmacol.* **2021**, *891*, 173759. [Crossref]
17. Hamid, S.; Mir, M. Y.; Rohela, G. K.; *New Microbes New Infect.* **2020**, *35*, 100679. [Crossref]
18. Mukherjee, P.; Shah, F.; Desai, P.; Avery, M.; *J. Chem. Inf. Model.* **2011**, *51*, 1376. [Crossref]
19. Xiang, Y.; Wang, M.; Chen, H.; Chen, L.; *Biochem. Pharmacol.* **2021**, *192*, 114724. [Crossref]
20. Konwar, M.; Sarma, D.; *Tetrahedron* **2021**, *77*, 131761. [Crossref]
21. Pillaiyar, T.; Manickam, M.; Namasivayam, V.; Hayashi, Y.; Jung, S.-H.; *J. Med. Chem.* **2016**, *59*, 6595. [Crossref]
22. Chen, L.-H.; Wang, Y.-C.; Lin, Y. W.; Chou, S.-Y.; Chen, S.-F.; Liu, L. T.; Wu, Y.-T.; Kuo, C.-J.; Chen, T. S.-S.; Juang, S.-H.; *Bioorg. Med. Chem. Lett.* **2005**, *15*, 3058. [Crossref]
23. Zhou, L.; Liu, Y.; Zhang, W.; Wei, P.; Huang, C.; Pei, J.; Yuan, Y.; Lai, L.; *J. Med. Chem.* **2006**, *49*, 3440. [Crossref]
24. Liu, M.; Qiu, S.; Ye, Y.; Yin, G.; *Tetrahedron Lett.* **2016**, *57*, 5856. [Crossref]
25. Zhao, P.; Li, Y.; Gao, G.; Wang, S.; Yan, Y.; Zhan, X.; Liu, Z.; Mao, Z.; Chen, S.; Wang, L.; *Eur. J. Med. Chem.* **2014**, *86*, 165. [Crossref]
26. Araújo, D. B.; Machado, R. R. G.; Amgarten, D. E.; Malta, F. M.; de Araujo, G. G.; Monteiro, C. O.; Candido, E. D.; Soares, C. P.; de Menezes, F. G.; Pires, A. C. C.; Santana, R. A. F.; Viana, A. O.; Dorlass, E.; Thomazelli, L.; Ferreira, L. C. S.; Botosso, V. F.; Carvalho, C. R. G.; Oliveira, D. B. L.; Pinho, J. R. R.; Durigon, E. L.; *Mem. Inst. Oswaldo Cruz* **2020**, *115*, e200342. [Crossref]
27. Freire, M. C. L. C.; Noske, G. D.; Bitencourt, N. V.; Sanches, P. R. S.; Santos-Filho, N. A.; Gawriljuk, V. O.; de Souza, E. P.; Nogueira, V. H. R.; de Godoy, M. O.; Nakamura, A. M.; Fernandes, R. S.; Godoy, A. S.; Juliano, M. A.; Peres, B. M.; Barbosa, C. G.; Moraes, C. B.; Freitas-Junior, L. H. G.; Cilli, E. M.; Guido, R. V. C.; Oliva, G.; *Molecules* **2021**, *26*, 4896. [Crossref]
28. Sales-Medina, D. F.; Ferreira, L. R. P.; Romera, L. M. D.; Gonçalves, K. R.; Guido, R. V. C.; Courtemanche, G.; Buckeridge, M. S.; Durigon, E. L.; Moraes, C. B.; Freitas-Junior, L. H.; *BioRxiv* **2022**. [Crossref]
29. *GraphPad Prism*, version 9.0; GraphPad Software, San Diego, USA, 2022.
30. Liu, P.; Liu, H.; Sun, Q.; Liang, H.; Li, C.; Deng, X.; Liu, Y.; Lai, L.; *Eur. J. Med. Chem.* **2020**, *206*, 112702. [Crossref]
31. Badavath, V. N.; Kumar, A.; Samanta, P. K.; Maji, S.; Blum, D. A.; Jha, G.; Sen, A.; *J. Biomol. Struct. Dyn.* **2022**, *40*, 3110. [Crossref]
32. Varadharajan, V.; Arumugam, G. S.; Shanmugam, S.; *J. Biomol. Struct. Dyn.* **2022**, *40*, 7872. [Crossref]

Submitted: August 11, 2022

Published online: November 8, 2022

